DOE/NASA/10769-25
NASA TM-82864

Results and Comparison of Hall and DW Duct Experiments

J. Marlin Smith and J. L. Morgan
National Aeronautics and Space Administration
Lewis Research Center

Work performed for
U.S. DEPARTMENT OF ENERGY
Fossil Energy
Office of Magnetohydrodynamics

Prepared for
Twentieth Symposium on Engineering
Aspects of Magnetohydrodynamics
Los Angeles, California, June 14-16, 1982

DOE/NASA/10769-25
NASA TM-82864

Results and Comparison of Hall and DW Duct Experiments

J. Marlin Smith and J. L. Morgan
National Aeronautics and Space Administration
Lewis Research Center
Cleveland, Ohio 44135

Work performed for
U.S. DEPARTMENT OF ENERGY
Fossil Energy
Office of Magnetohydrodynamics
Washington, D.C. 20545
Under Interagency Agreement DE-AI01-77ET10769

Prepared for
Twentieth Symposium on Engineering
Aspects of Magnetohydrodynamics
Los Angeles, California, June 14-16, 1982

RESULTS AND COMPARISON OF HALL AND DW DUCT EXPERIMENTS*

J. Marlin Smith and J. L. Morgan
NASA-Lewis Research Center
Cleveland, Ohio

Abstract

Experimental data from recent tests of a 45° diagonal wall duct are presented and compared with the results of a similar Hall duct. For the results obtained here it is shown that while the peak power density of the two devices is approximately equal that the diagonal wall duct produces greater total power output due to its ability to better utilize the available magnetic field.

I. Introduction

In this paper the results of recent tests utilizing a diagonal wall (DW) MHD duct with a diagonalization angle of 45° are presented and compared with the results of a similar Hall duct. The experiments were run in the NASA-Lewis high magnetic field strength, liquid-neon-cooled cryomagnet facility (ref. 1), which has been modified to run under vacuum exhaust through the addition of a large vacuum tank (ref. 2). This tank allows evacuation of the system to approximately 2 psia and has sufficient capacity to maintain an exhaust pressure of less than 1/2 atmosphere during the duration of a 5 sec run.

II. Duct Construction

Hall Duct

The heat sink Hall duct has been described previously (ref. 2). Briefly, it is made up of 5 modules each consisting of 16 circular electrodes clamped by 3 electrically isolated stainless steel tie bolts between 2 triangular electrodes at each end for a total of 20 electrodes/module. The copper electrodes are .64 cm wide and electrically insulated from one another by a high temperature asbestos gasket .078 cm thick (to provide the pressure seal), sandwiched between two .013 cm thick sheets of mica (to provide the electrical insulation and moisture barrier). Lateral movement of the electrodes is negated by three fiberglass rods inserted through the entire module. Five such modules are used in the present experiments with 2.22 cm thick end flanges for a total of 102 electrodes having a total length of approximately 78 cm. The duct is conically bored from a 4.95 cm inlet diameter to a 12.4 cm outlet diameter.

DW Duct

The construction of the 45° DW duct is philosophically the same as the Hall duct, i.e., modules clamped with stainless rods and shear movement negated by fiberglass rods. The duct consists of 4 modules of 11 electrodes each. The thickness of the electrodes is 1.25 cm so that the segmentation pitch is approximately twice that of the Hall duct. The DW duct was also restricted by design limitations to a somewhat smaller overall area ratio than the Hall duct and therefore was conically bored from a 4.95 cm inlet diameter to a 9.91 cm diameter at a distance of 57.8 cm from the entrance. The remainder of the duct was kept at this diameter. The total length of the duct was 80.2 cm and it was located within the magnet bore tube so as to best approximate the area ratio of the Hall duct over the active region of the Hall duct. The location of the two ducts relative to the centerline of the magnet and their internal outlines are shown in figure 1.

III. Power Takeoff Location

It is noted from figure 1 that the power producing region for the DW duct is considerably larger than that of the Hall duct. This is the result of the maximum power location of the power leads for the single load resistance configuration used in these experiments. In figure 2 the axial profile of Hall voltage as a function of distance from the magnet centerline is shown. In both curves the load was connected across the first and last electrodes. This power takeoff location leads to regions of power dissipation, as noted by the negative slope of the voltage curve at the front and rear of the ducts. Therefore to obtain the maximum power output with a single load, the power takeoffs must be located at the front and rear min-max points of the voltage curve. From figure 2 it is seen that these points cover a much larger portion of the magnetic field region for the DW duct than for the Hall duct.

The reason for the above difference is seen from the equation for the Hall electric field (ref. 3)

$$E_x = \frac{(1+\beta^2)\,I}{\sigma A\,(1+\phi^2)} - \frac{(1-\Delta)(\beta+\phi)uB}{1+\phi^2} \qquad (1)$$

where A is the cross sectional area of the duct and u is the local gas velocity, B is the magnetic field intensity, σ is the electrical conductivity, β is the Hall parameter, Δ is the dimensionless effective voltage drop, I is the load current and ϕ is the tangent of angle between the direction of $u\times B$ and the plane of the electrode, i.e., $\phi = 0$ for Hall duct and 1 for 45° DW duct. Therefore,

$$E_{x\,Hall} = \left[\frac{1+\beta^2}{\sigma A}\right] I - \beta(1-\Delta)uB \qquad (2)$$

$$E_{x\,DW} = \frac{1}{2}\left[\frac{1+\beta^2}{\sigma A}\, I - (1+\beta)(1-\Delta)uB\right] \qquad (3)$$

*Work done under DOE/NASA Interagency Agreement No. DE-AI01-77ET10769.

The min-max point occurs for for $E_x = 0$. Comparing equations 2 and 3, it is seen that the $(1 + \beta)$ multiplier of the EMF term for the DW duct is greater than the β multiplier for the Hall duct. Therefore, other things being equal, the inflection point for the DW duct will occur at a lower B field than for the Hall duct. Hence a greater portion of the magnetic field region can be used by the DW duct with a single load resistance.

Based upon the above considerations, the load resistance was connected between electrodes 12, 13, 14 to electrodes 42, 43, 44 for the DW duct and between electrodes 38, 39, 40 to electrodes 90, 91, 92 for the Hall duct.

IV. Load Considerations and Power Output

Figure 3 shows the voltage-current relationships for the Hall and DW duct. The slope of these VI curves, of course, represent the total internal impedance of the device. From these curves it is found that the internal impedance is 19.8 ohm and 29.9 ohm for the DW duct and the Hall duct, respectively. This difference in impedance can be shown to be consistent with theory. The theoretical value of the impedance from equation 1 is taken from the first term on the right of equation 1 to be

$$R = \frac{1}{1+\beta^2}\int_0^L \frac{1+\beta^2}{\sigma A}\,dx \qquad (4)$$

where L is the active length of the duct.

To first order the plasma properties of the two devices are equal (low power extraction in both devices, i.e., max. enthalpy extraction = 3.5 percent) and therefore from equation 4 their impedances should ratio approximately like

$$\frac{R_{Hall}}{R_{DW}} \approx \frac{L_{Hall}}{\frac{1}{2}L_{DW}} = \frac{2\ (37.5\ cm)}{51.75\ cm} = 1.45 \qquad (5)$$

where the active lengths were obtained from figure 1. This result compares favorable with that obtained from the V-I curves, i.e.,

$$\frac{R_{Hall}}{R_{DW}} = \frac{29.9\ ohm}{19.8\ ohm} = 1.51 \qquad (6)$$

In the discussion to follow, all of the data was taken with a load resistance of 11.5 ohm while for peak power output one wants to match the internal impedance. The reason for the choice of 11.5 ohm was the present voltage isolation limitation upon some of the instrumentation which would be exceeded at the upper limits of the magnetic field strength (5 tesla). This clearly favors the performance of the DW duct since it is a lower impedance device.

In figure 4 the power output of the two devices is shown as a function of the square of the B-field. It is seen, as has been previously observed over a broad range of Hall duct area ratios (ref. 4), that the power output of the Hall duct is linear with the square of the magnetic field. This is also true of the DW duct up to approximately 4 tesla beyond which the rate of increase in power output with the square of the magnetic field decreases. This characteristic was also observed for Hall ducts when the pressure ratio across the duct was insufficient to provide shock free performance throughout the duct (ref. 4). For the circled points of the DW duct curve the scatter in the pressure data was sufficient that the presence of a shock could not be detected. However, for the square point labeled "Run 564" (the 4 square points on figure 4 represents runs made at the fuel rich oxygen/fuel weight ratio of 6/1) the presence of a shock was detected.

In figure 5 the time dependence of the Hall voltage is plotted for Run 564. It is seen that at a time of between 3.2-3.4 sec there is an abrupt decrease in the Hall voltage. In figure 6 the axial pressure profile is plotted. The curve drawn through the circled points represents the profile just prior to the Hall voltage decrease. In this case no abrupt increase in pressure is observed although the adverse pressure gradient at the rear of the duct could possibly indicate a weak shock. The square points represent the pressure profile after the Hall voltage decrease and definitely indicates the presence of a shock in the neighborhood of electrode 24. This can also be seen from the Hall voltage axial profile shown in figure 7. In this figure shock location corresponds to an "abrupt" change in the slope of the voltage profile in the neighborhood of electrode 24.

The time dependency for the creation of the shock is due to the buildup of back pressure in the vacuum tank during the run (the vacuum pump is too small to maintain vacuum pressure while the combustor is running). In the early stages of the run, it is suspected that the shock is located at the exit of the diffuser. When the back pressure increases to a point where there is insufficient pressure ratio across the duct then the shock moves through the constant area diffuser and downstream portion of the DW duct into the conical portion of the duct (upstream of electrode 33) where it can stably attach for the remainder of the run.

The point labled "Run 564" on figure 4 is the value prior to the shock induced decrease in the Hall voltage and represents the largest power extraction yet attained in our facility representing 275 kW which is 3.5 percent of the input enthalpy. Also from figure it is noted that the voltage sustained without electrical breakdown was 90 V/insulator. This represents a substantial increase over the 50 V/insulator value observed for a Hall duct with similar segmentation ratio (ref. 1). The Hall duct discussed in the present paper has a segmentation ratio 1/2 that of the DW duct and no electrical breakdown has been observed in this duct.

In figure 8 the axial profile of power density for the Hall and DW duct is shown. The interesting point is that the peak power densities are nearly equal and therefore the higher power output of the DW channel is primarily due to its better utilization of the magnetic field in the end regions.

V. Concluding Remarks

Specific conclusions that may be drawn from the comparison of the DW and Hall ducts studied in this paper is that;

1. Singly loaded DW ducts can utilize more of the magnetic field region than can Hall ducts.

2. Hall ducts are higher impedance devices.

3. Although interelectrode electrical breakdown was not specifically studied for the DW duct voltages of 90 V/insulator were obtained with no breakdown. This is substantially higher than the 50 V/insulator which was previously observed for a Hall duct of similar segmentation ratio.

References

1. Smith, J. M.: Preliminary Results in the NASA Lewis H2-02 Combustion MHD Experiment. Proceedings of the 18th Symposium on the Engineering Aspects of Magnetohydrodynamics, Butte, Montana, June 1979, pp. A.2.1-A.2.6.

2. Smith, J. M.; Morgan, J. L.; and Wang, S. Y.: Effects of Vacuum Exhaust Pressure on the Performance of MHD Ducts at High B-Field. AIAA Paper 82-0396, Jan. 1982.

3. Wu, Y. C. L.: Performance Theory of Diagonal Conducting Wall MHD Generators. AIAA, vol. 14, no. 10, Oct. 1976, pp. 1362-1368.

4. Smith, J. M.; Wang, S. Y.; and Morgan, J. L.: High B-Field, Large Area Ratio MHD Duct Experiments. 1981 IEEE International Conference on Plasma Science, Santa Fe, New Mexico, Paper No. 1F6, May 1981.

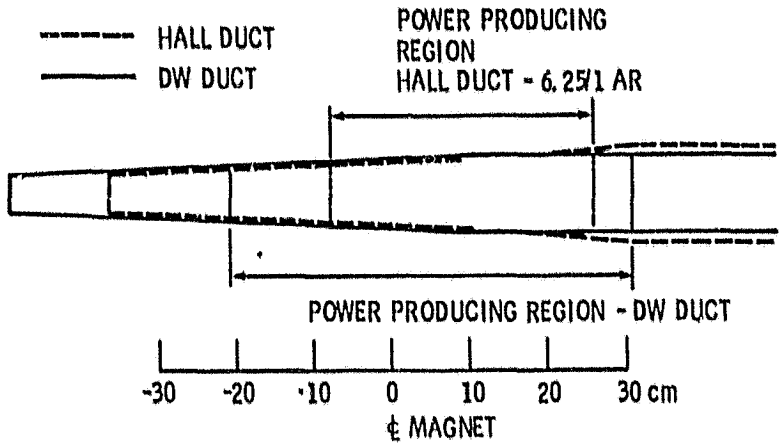

Figure 1. - Interior crossections of Hall and DW duct.

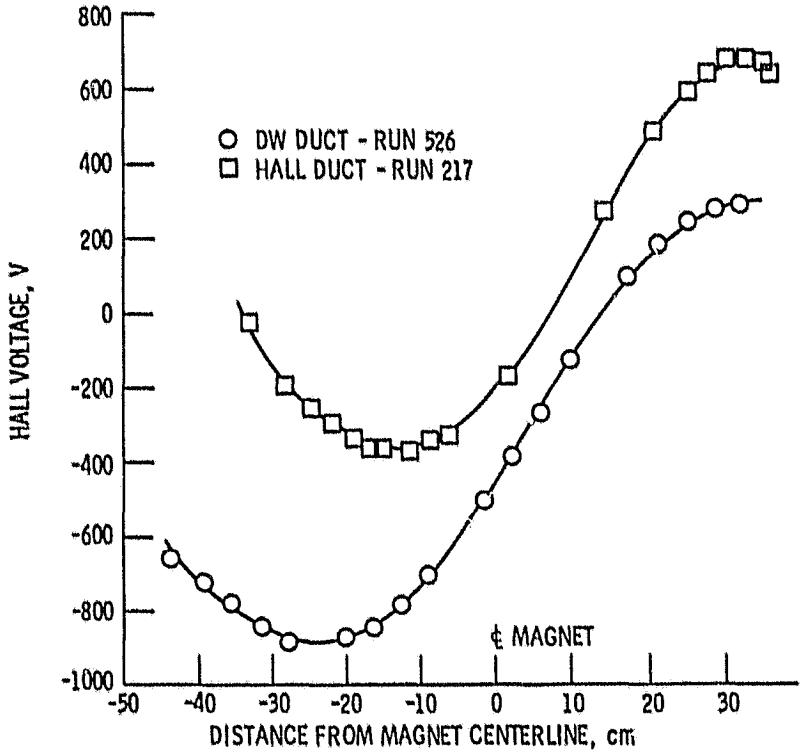

Figure 2. - Hall voltage profiles for determining power takeoff location.

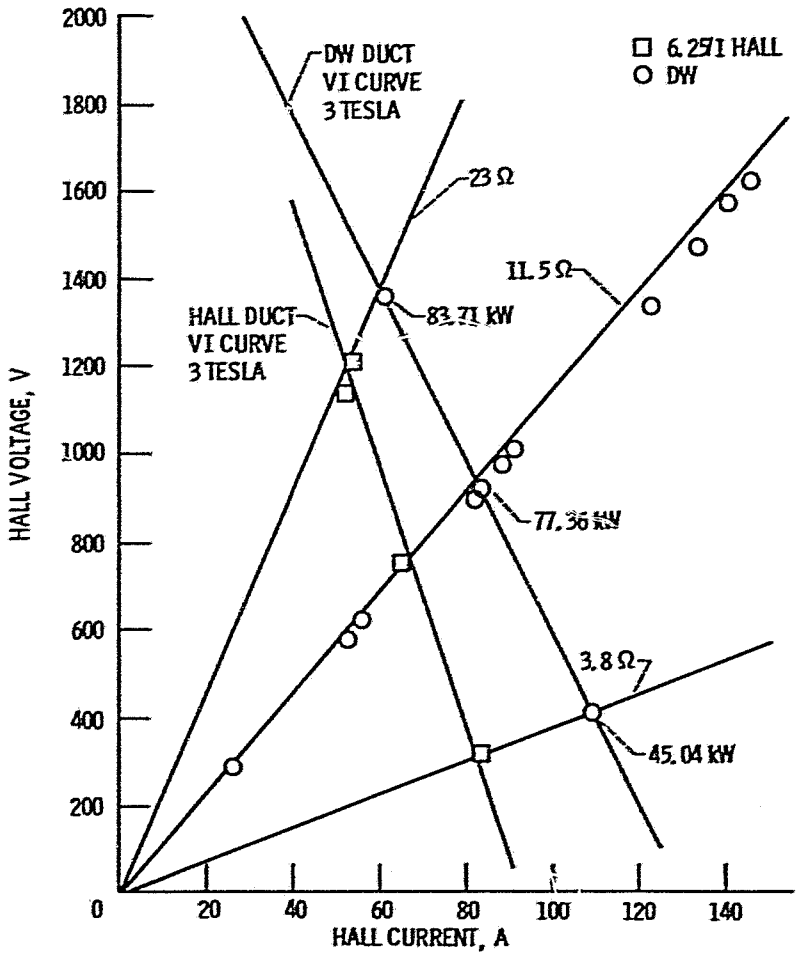

Figure 3. - Current voltage diagram.

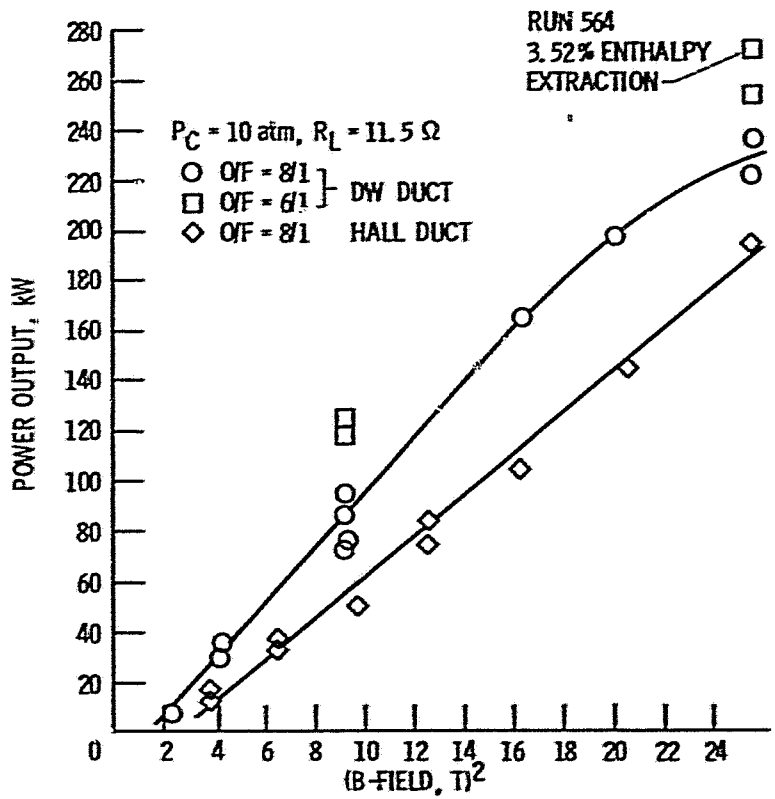

Figure 4. - Power output versus B-field squared.

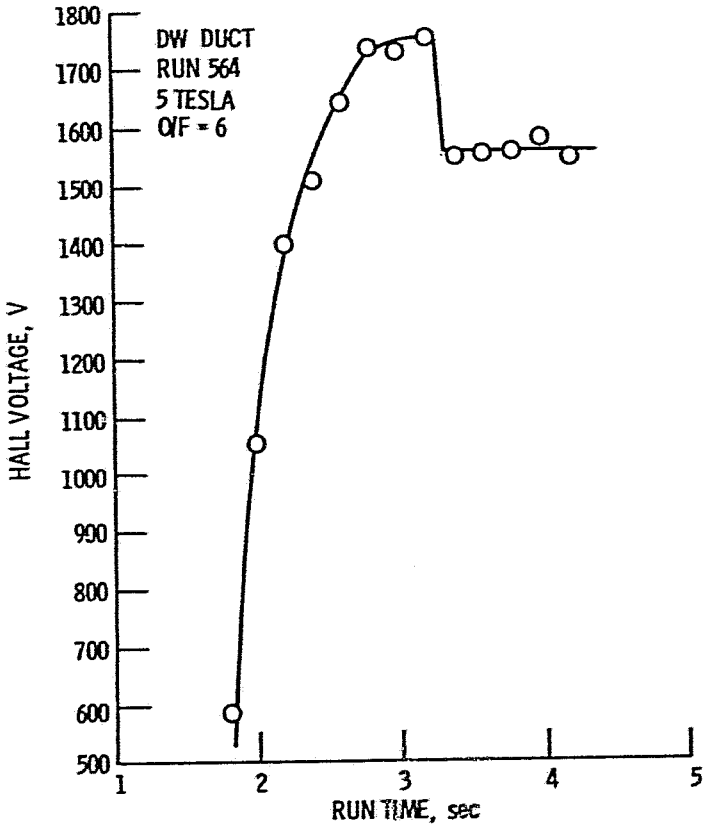

Figure 5. – Hall voltage as a function of time.

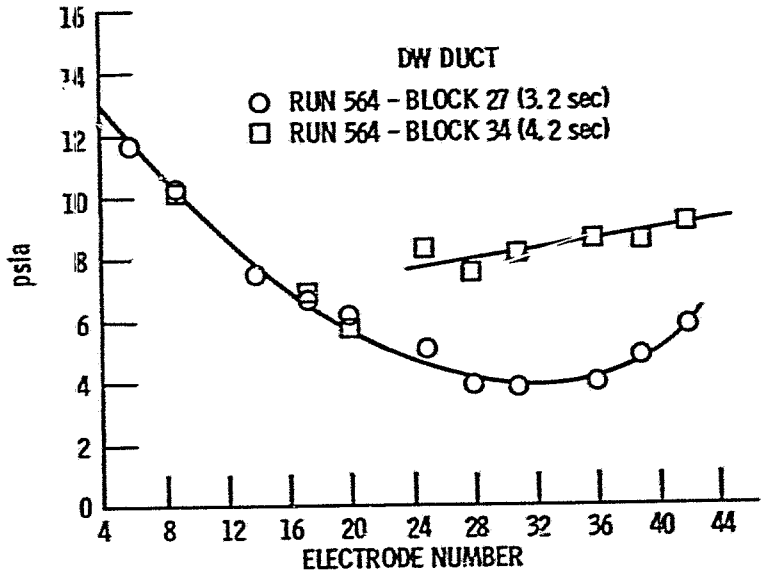

Figure 6. – Axial pressure profile.

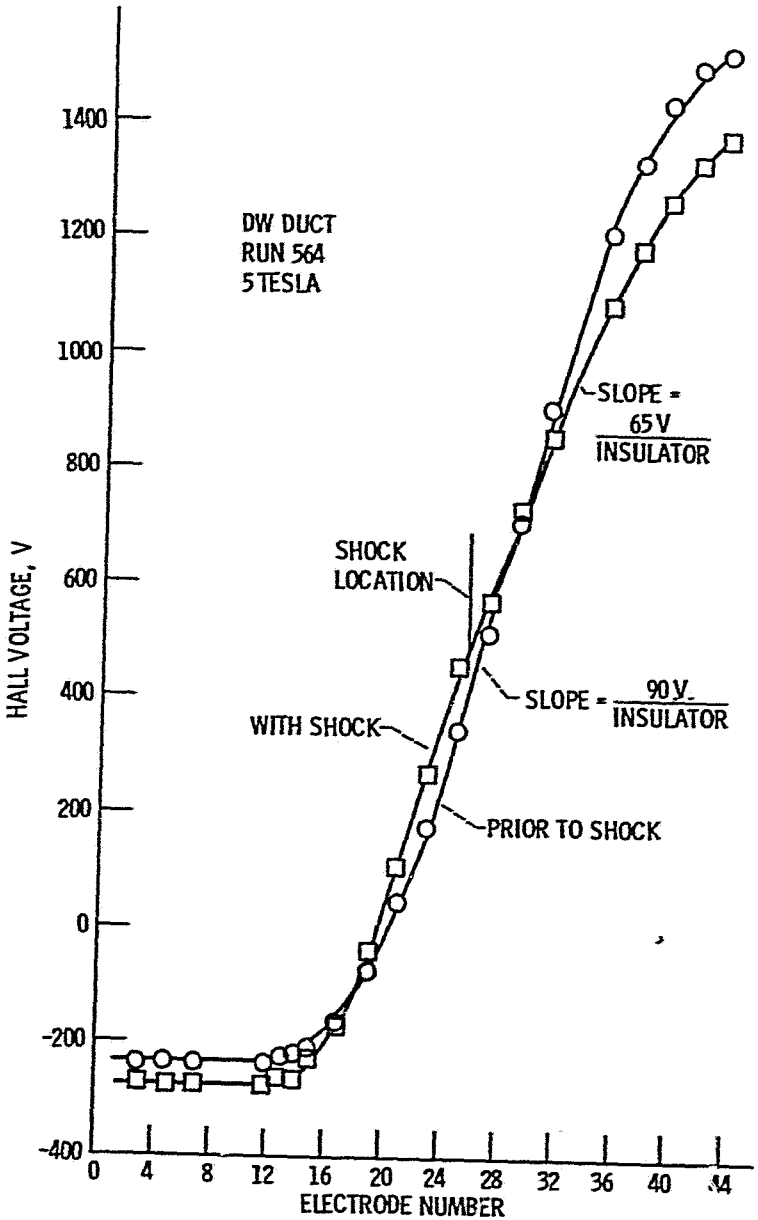

Figure 7. – Axial hall voltage profile.

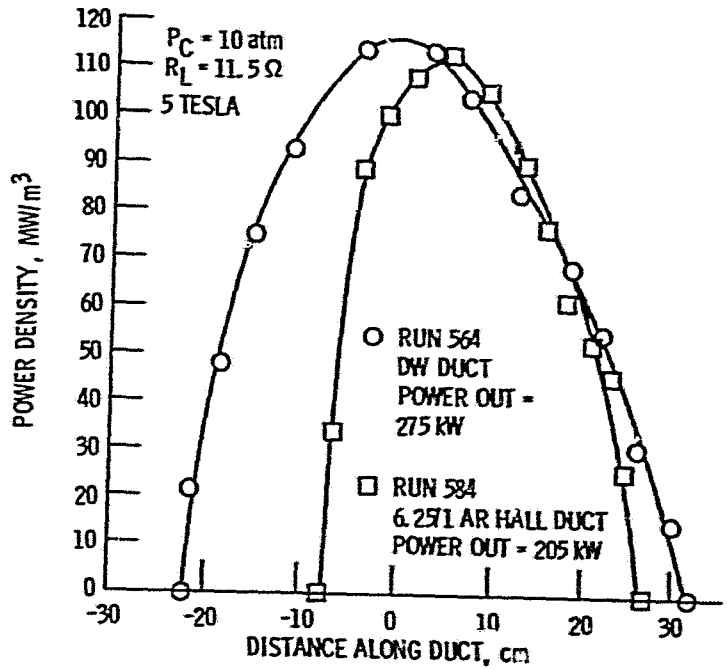

Figure 8. – Axial power density profile.